CBN 13-5 March 23 2013

IRON-FREE DETECTORS FOR HIGH ENERGY PHYSICS

Alexander Mikhailichenko, Cornell University, Ithaca, NY

Abstract. We considered some peculiarities of magnetic system of Iron-free detector for High Energy collider.

INTRODUCTION

Longitudinal field at Interaction Point (IP) of any collider has a high level required by proper identification of momenta of the secondary particles generated at IP. Typically, magnetic field created with the help of superconducting solenoid with induction of 4T (ILD)-5T (SiD). Magnet yoke of detectors for colliders have tens of thousand tons of Iron to re-direct the magnetic field flux from the one end of solenoid to the opposite one. From the other hand it is known, that the magnetic field value outside of the (long) solenoid is zero. Solenoids used (or suggested for use) have some remaining field outside, depending on the length/diameter ratio. In practice, the iron adds ~20% of the field value in a realistic geometry only. With invention of calorimeters which are able to determinate the type of particle (so-called dual readout calorimeters), identification of muons, carried usually with the help of back leg yoke iron, interlaced by muon identification system, is now transferred to the calorimeter itself.

In this communication we represent the basic principles put in grounds of iron-free detector. In such detector the magnetic flux is closed with the help of additional solenoid(s). Stray field outside detector has minimal level with implementation of end coils. With elimination of iron yoke the detector becomes lightweight and easy accessible for further modifications. Engineering realization and some technologies associated with such detector, suggested for ILC (4-th Concept) described in detail.

We are projecting parameters of such detector for usage with a few TeV-scale colliding beams which inevitably will appear in a future.

OVERVIEW

The steel yoke of any contemporary detector for High-Energy physics impresses everyone who had a chance to see it.

Structurally the detector consists on few main elements such as:

1) Pixel vertex detector for high-precision identification of vertex,
2) Drift Chamber for 3D restoration of tracks,
3) Calorimeter for the energy measurement of hadrons, jets, electrons, photons, missing momentum, and the tagging of muons and other particles.

Longitudinal magnetic field well fits into axial symmetry of colliding beams. So the magnetic field value defined by the required momentum resolution, which is

$\Delta p / p \sim 1/(B_0 D^2)$ where B_0 stands for the central field in a central solenoid, D is its diameter. Typical detector cross section represented in Fig.1.

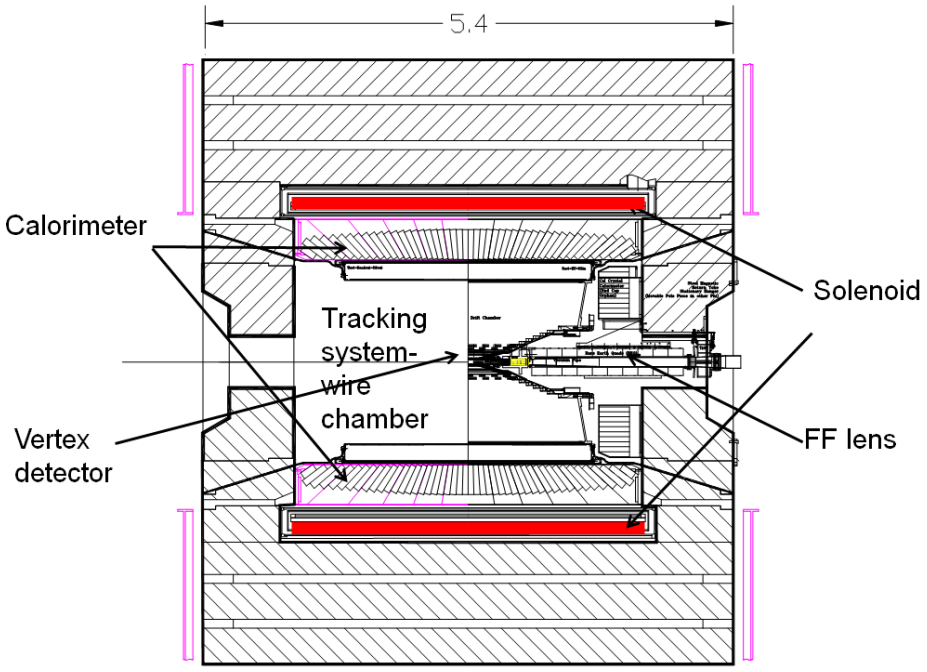

Figure 1. Typical mid-size detector (CLEO; operated for ~5GeV beams). Dimension is given in meters. Magnet yoke is hatched. If permeability of Iron put to a one, the field at the center will be 25% lower for this particular geometry.

The main role of this magnet yoke is the service as a duct for the return flux of main (central) solenoid. If the yoke magnetic permeability changed to the one (Air), the field inside a solenoid drops about 25% only for a typical detector from Fig.1, [1]. Mostly this change impacts the field homogeneity. This drop associated with the finite ratio of the length of main solenoid to its diameter. It is well known that there is no significant field outside of long solenoid. Field outside has strictly zero value for (infinitely) long one. Also, the field is homogenous inside the (long) solenoid. So bigger the Length/diameter ratio-lesser the drop is.

Having a good field homogeneity in a region where the tracking system located, required for the tracks identification be easier. With a Cluster Counting *CluCou* technology [2], see belw, the homogeneity required could be less than in the Time Projection Chamber (TPC), however. The productivity of contemporary processors dedicated to this job, allow corrections for the field inhomogeneity to be done in a real time.

In addition, detectors have (superconducting) final quads inside the magnet field of detector and theirs field have significant value in a region where the wire chamber located. This makes trajectory analysis more complicated also. Detector physicists are prepared for this and are ready to make all necessary corrections, however (what indicates a potential for further developments).

Thinking ahead, with some novel accelerator techniques, see for example [3], one should see a possibilities for detectors, having multi-hundred GeV colliding particles. These detectors will require as high field in central region as possible with maximal possible diameter of central solenoid. One can count on implementation of 10-20 T fields in central SC solenoid. Meanwhile the iron becomes deeply saturated at the field level ~2T, so the magnetic yoke of a traditional detector will be saturated even for the field level 3T.

THE CONCEPT OF IRON-FREE DETECTOR

The yoke is an element of the magnet circuit only, so anyone can consider its elimination. For realistic diameter/length ratio homogeneity of field in a central region will drop, naturally.With additional ampere-turns at the end region of superconducting solenoid (Helmholtz) the field can be made homogenous again at any level required. Additional heat and electricity losses are negligible. These additional turns can be located, naturally, inside the same cryostat. Few possibilities become open for Iron free detector design. A family of Iron-free detectors is represented in Fig.2. It starts from just a single, solenoid, a). This single-solenoid system is inexpensive, compact, but it generates significant stray-field in outer space. This stray field requires attention, but could be screened by relatively thin sheets of iron. Dual solenoid system b) is much better in this aspect. One minus of dual solenoidal system is that the field of outer solenoid, having opposite to the main solenoid polarity reduces the field in a central region. Next member of this family is a triple solenoid system c). Here two outer solenoids have opposite polarities, so there is no reduction of field. The field between the inner (first) and the second solenoid is about zero, i.e. free space. Minus of this system is that it requires additional solenoid. And the last member of family is a multiple-return solenoids one, d). This type requires fabrication of many solenoids, but as diameter of solenoids are small, these ones could be fabricated with much less effort, than the additional solenoid in b).

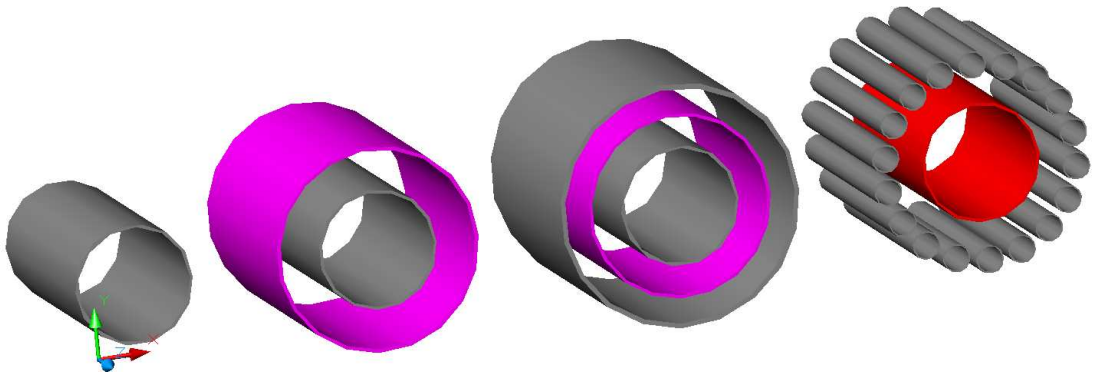

a) b) c) d)

Figure 2. A family of Iron-free detectors: a)-single solenoid, b)-dual solenoids, c)-triple solenoids, d)- many return-flux solenoids. Each system of solenoids surrounded by the end-cap-wall of coils (which are not shown here, see Fig.4).

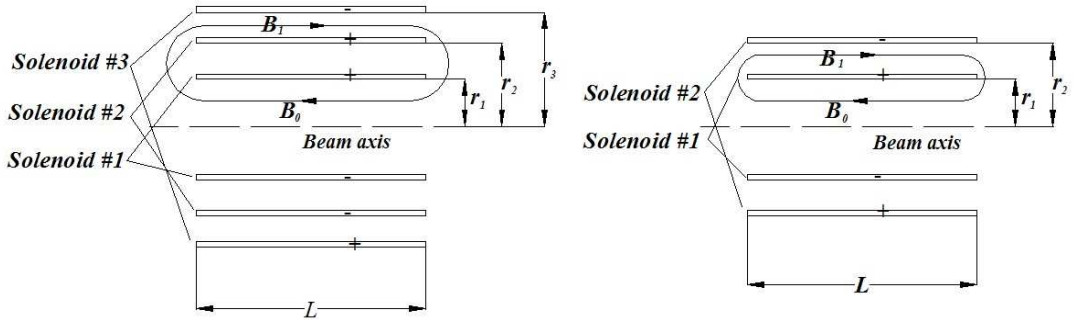

Figure 3. Geometry of three–coil system, left. At the right there is represented the situation when two coils from the left figure merged together (r_1=r_2). Signs "+" and "–" indicate direction of solenoidal current circulating in the coil.

Magnetic field and the current in each solenoid can be found from the simple condition

$$B_0 \times r_1^2 = B_1 \times (r_3^2 - r_2^2) \ , \tag{1}$$

which is just a reflection of conservation of the flux. When two coils merge together, the last formula simplified to the following

$$B_0 \times r_1^2 = B_1 \times (r_2^2 - r_1^2) \ , \tag{2}$$

Magnetic field $B \cong NI / L$, where *NI* stands for the total current running in the coil. So the volume between coils at r_1 and r_2 (solenoid 2 and 1) can be made practically free from magnetic field. The last circumstance might be useful in some cases.

Let us estimate the fields ratio for typical values which are $r_1 \cong 2.5$m, $L \cong 5$ m , $B_0 \cong 5$ T. So if $r_2 \cong 4$m (1.5 m radial space between inner solenoid and the next one), $r_3 \cong$ 5m, then in first case (thee coils), magnetic field value in return space between solenoid 3 and 2 comes to

$$B_1 = B_0 \frac{r_1^2}{r_3^2 - r_2^2} \cong 5 \frac{2.5^2}{5^2 - 4^2} \cong 3.5\,\mathrm{T} \tag{3}$$

and in the second case (two coils) magnetic field goes to

$$B_1 = B_0 \times \frac{r_1^2}{r_2^2 - r_1^2} \cong 5 \times \frac{2.5^2}{4^2 - 2.5^2} \cong 3.2\,\mathrm{T} \tag{4}$$

One can easily scale these figures to any appropriate radii. One might consider the placement of two outer solenoids practically at the outer housing of detector.

Field outside of solenoid drops rapidly as it was shown in [1]. Basically magnetic field drops as a third power of the distance *R*,

$$\vec{H} = \frac{3\vec{n} \cdot (\vec{n} \cdot \vec{M}) - \vec{M}}{R^3}, \tag{5}$$

where $\vec{n}$ is unit vector in direction of *R*, and $\vec{M}$ is the magnetic moment of solenoid,

$$\vec{M} = \frac{1}{2c} \int (\vec{j} \times \vec{r}) dV = \frac{\pi r^2 J}{2c}, \tag{6}$$

J is total current, *r* is the radius of solenoid. Even at the distance of ~1-2 meters the fields naturally drops to ~0.5kG, where local iron shields can be implemented easily if necessary. Some local shielding far from the solenoid ends can be implemented easily.

We would like to remind that the Iron itself might cost $35M easily, one can refer to this number in publications at ILC web-site. The cost of detector with SC coils is much lower. At least one SC coil is present in any detector anyway, so the cost of other two must be compared with the cost of iron, its tooling, transportation, and installation.

Mostly impressive advantage of Iron-free detector is a functional flexibility, easy commissioning in addition to lowered cost. The last allows fabrication of two (or even more) detectors for experiments. We called this concept *modular detector*.

Field inside inner and outer solenoids (and between) can be made homogeneous to the level required by adding the wires at the end of each solenoid (Helmholtz-type coils). Optimization of such system takes very short time with appropriate code (MERMAID). Magnetic mapping allow proper reconstruction of trajectory practically with any field distribution, however.

The outer solenoids could be made segmented, so they will fill practically all volume, i.e. will be closer to triple solenoidal system, Fig.4

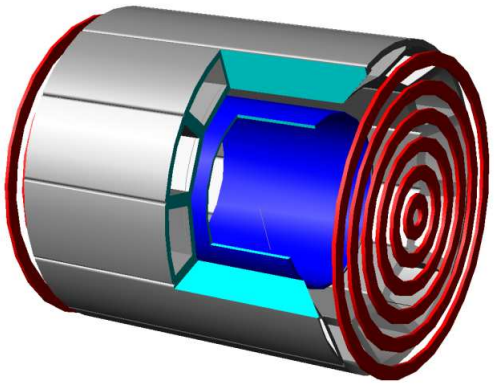

Figure 4. Many return-flux solenoids with the shape of segments for better coverage of volume with magnetic field.

4TH CONCEPT-DUAL SOLENOID SYSTEM

Detector developed for ILC by 4th concept team [9] is a bright representative of dual-solenoid family, b). This detector represented in Fig 5.

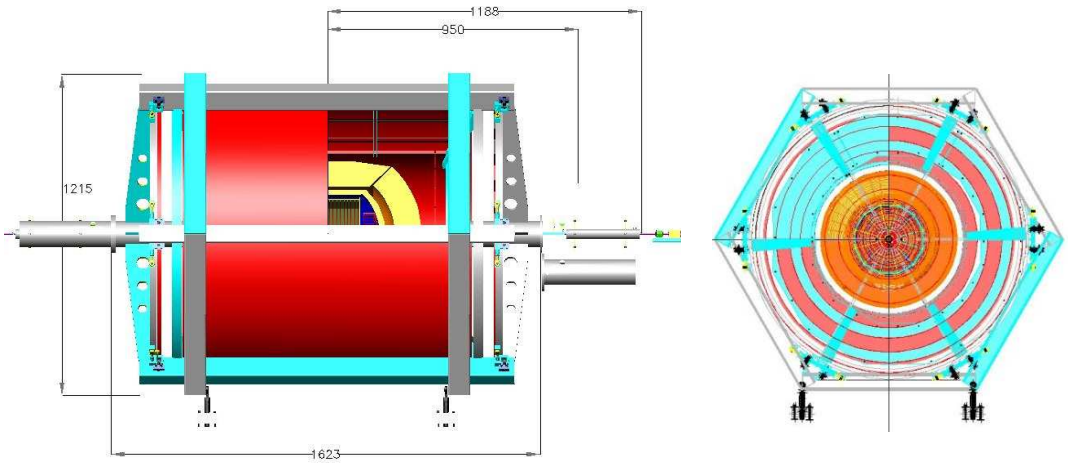

Figure 5. The 4th Concept detector suggested for ILC.

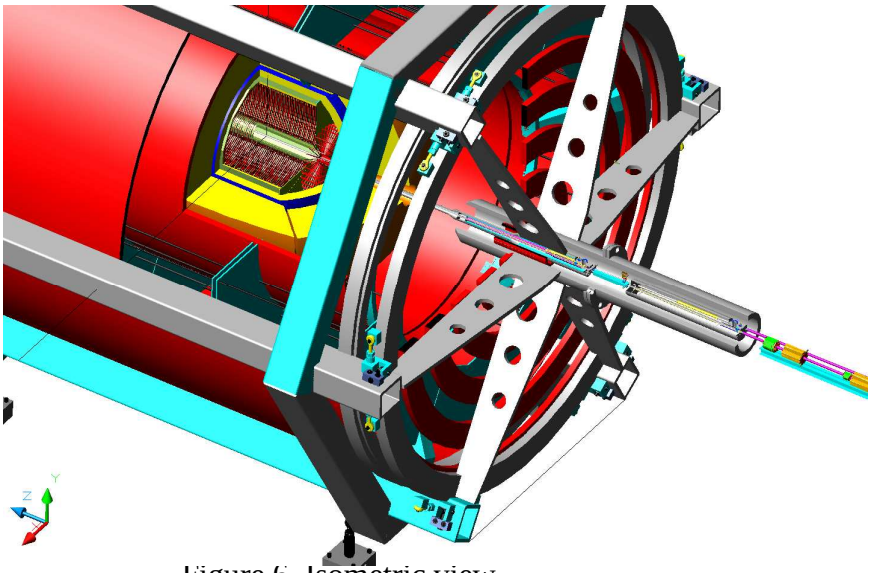

Figure 6. Isometric view.

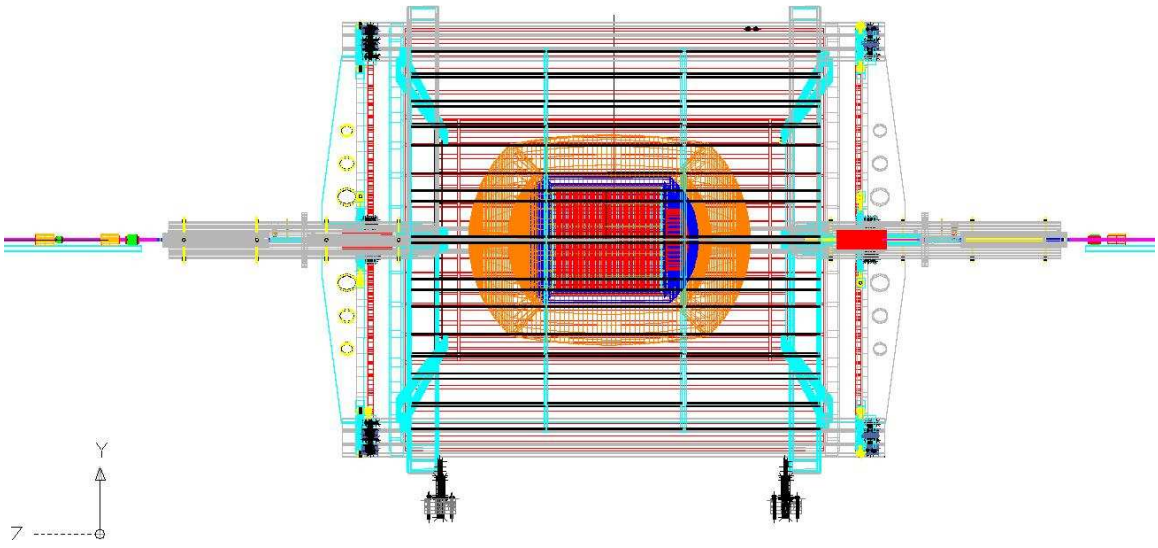

Figure 7. Transparent side view.

Main components of detector are represented in Fig. 7.

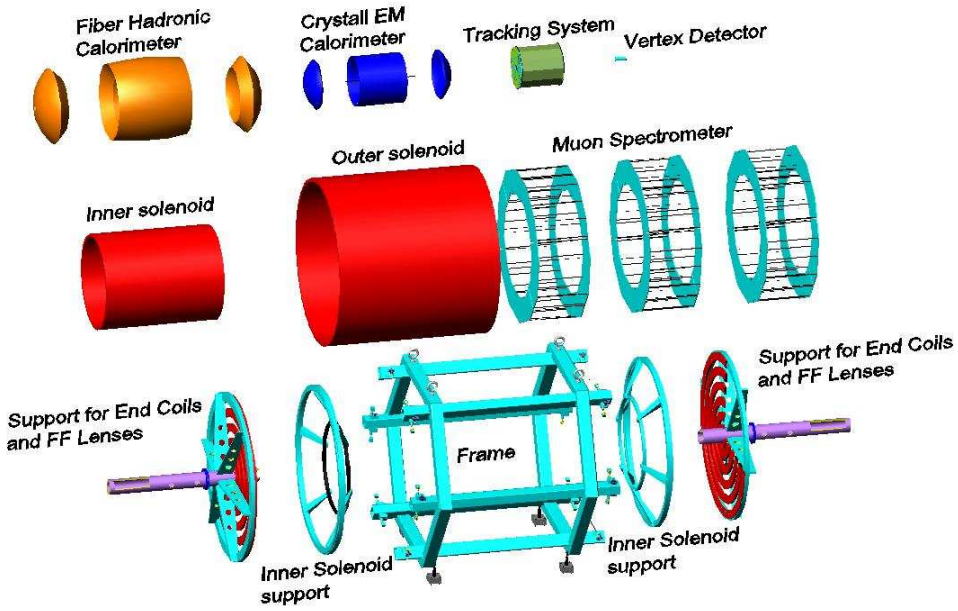

Figure 8. Main components of 4th Detector.

Magnetic field in detector.

Calculations of magnetic field were carried with help of MERMAID and FlexPDE codes.

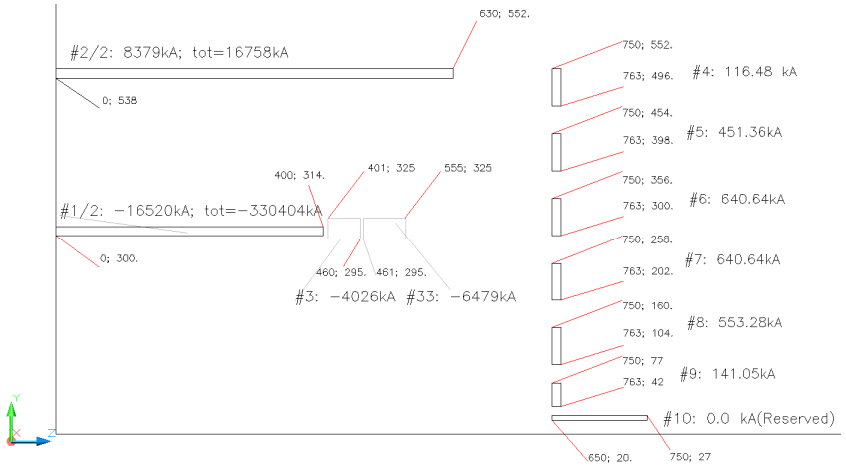

Figure 9. Locations and values of currents in 4th detector; ¼ of total cross section.

The total stored energy in a magnetic field ~2.77 *GJ*. Namely this energy should be evacuated if quench occurred.

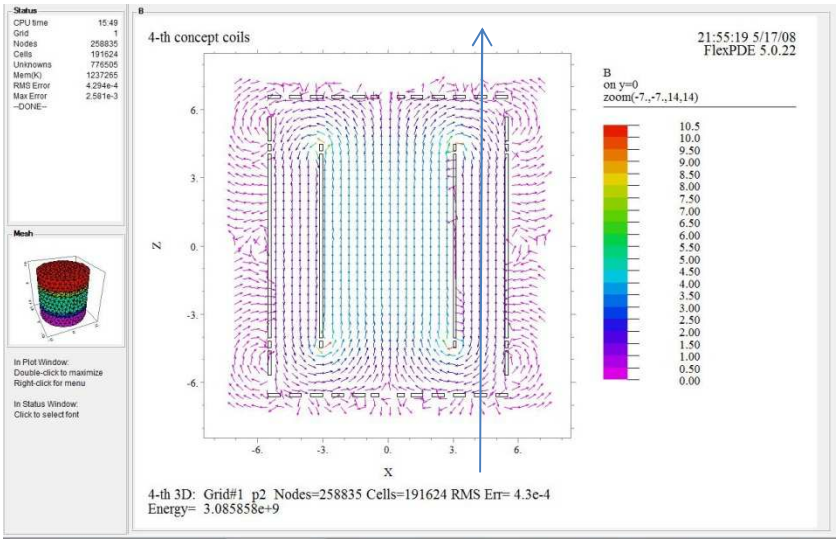

Figure 10. Vectors of magnetic field; full cross section. Arrow corresponds to the beam axis line.

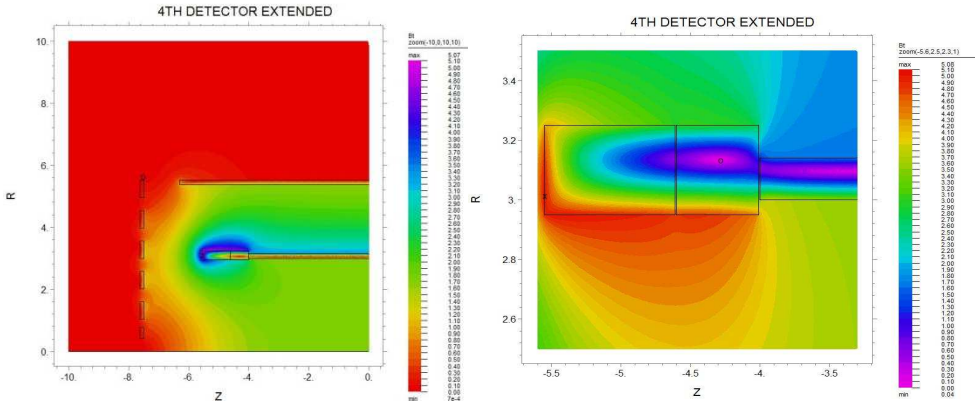

Figure 11. Contour plot of magnetic field module.

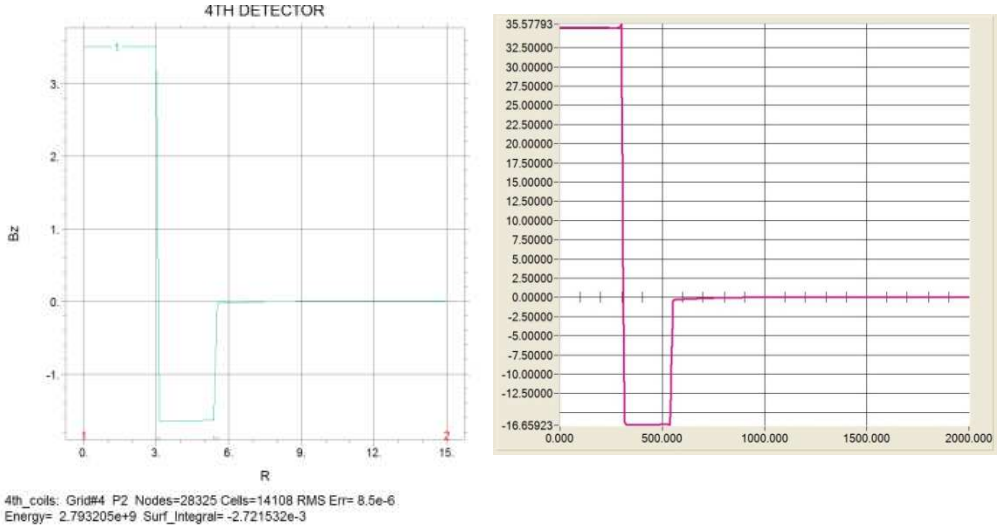

Figure 12. At the left: Radial distribution of longitudinal component of the field in a median plain; FlexPDE. At the right: The same distribution calculated with MERMAID. Field measuresd in Tesla.

All side coils are **room-temperature** ones; have ~same current density; water cooled. Current density in coils (from the smallest radius to the biggest): 1; 8; 4.2; 3.3; 3.7; 1.7 A/mm^2, corresponding longitudinal forces are: 1.75; 102; 131; 135; 111; 10 tons.

Field outside detector can be zeroed to any level by proper current distribution; Coils can be fixed easily at the end plates

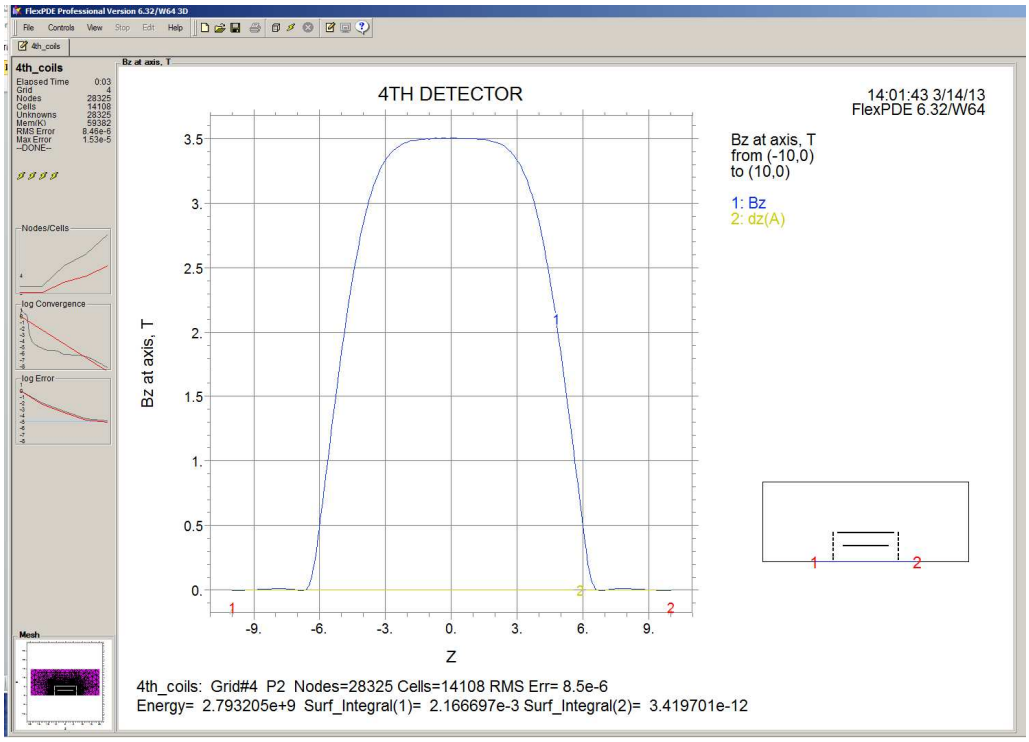

Figure 13. Longitudinal distribution of the field on axis. z- dimension is in meters, field in Tesla.

Space between solenoids used for muon spectrometry. Magnetic field level there is ~1.6 T. This space filled with many tubes filled with a mixture of Helium and Iso-Butane He +C_4H_{10} (90%+10%). Central wire of each tube for muon spectroscopy could be made from plated W. The number of tubes between solenoids comes to ~31500 tubes. The end caps contain 8640 tubes, Fig. 13.

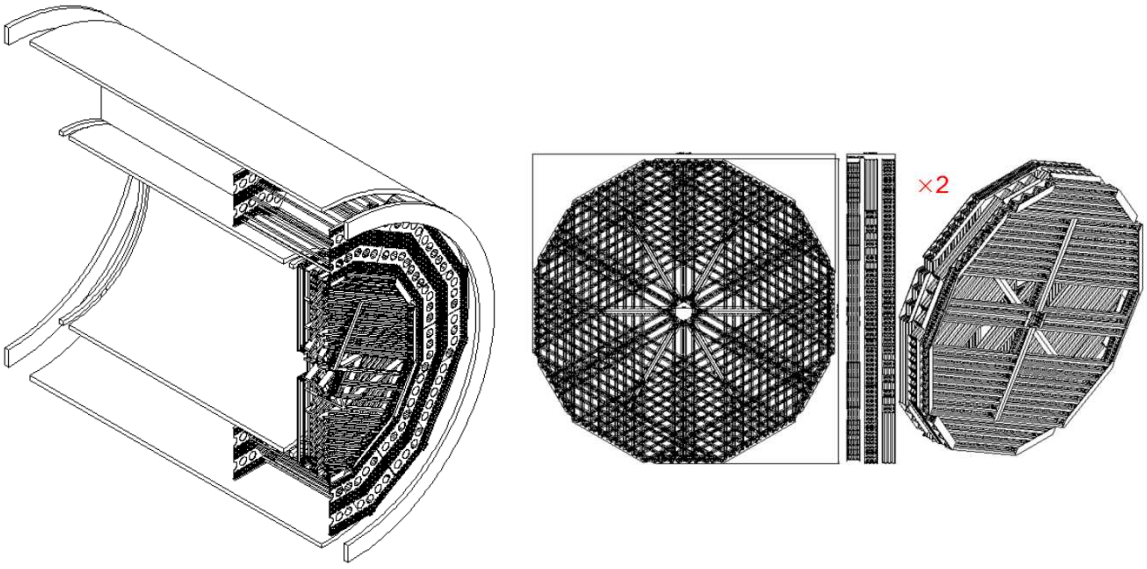

Figure 14. System of drift chambers between two solenoids (at the left). End caps magnified (at the right) [9].

MACHINE-DETECTOR INTERFACE (MDI)

Requirements for MDI underlined in [10]. One general requirement is that the Linear Collider should serve for at least for two different detectors, although there is no requirement that they should do this simultaneously (Push-Pull concept). We think that this concept will be useful for detectors working with multi-hundred TeV beams. Obviously, the off-beam line detector should be shifted shifted in transverse direction to a garage position, located 15m from the IP. The radiation and magnetic environment, suitable for people access to the off-beam line detector during beam collision, are to be guaranteed by the beam line detector using their chosen solution.

We anticipate that with development of more compact and, hence, less expensive Final Focus hardware, these two detectors can be served by beams at the same time on the basis of fast Switch Yard optics. In this case all the movement apparatus could be excluded, as the detectors stay in place.

***Basic principles of 4th, affecting* MDI**

• Beam-optical system incorporated in Detector

• Iron is omitted as it adds ~20% to the field value only (field outside of long solenoid is zero). Homogeneity restored by adding currents at the ends of main solenoid.

• Second solenoid closes the flux (minimal configuration).

• Muons can be identified with Dual (Triple) readout calorimeter scheme in more elegant way

Usage of dual solenoidal system plus end wall current system allows:

1) Strict confinement of magnetic field inside limited region.
2) Spectroscopy of muons in magnetic field between solenoids.
3) Incorporate FF optics in mostly natural way.
4) Modular design which helps in modifications and re-installations.
5) lightweight detector having flexible functionality and remarkable accuracy.
6) Easiest incorporation of laser optical system for gamma-gamma collisions.

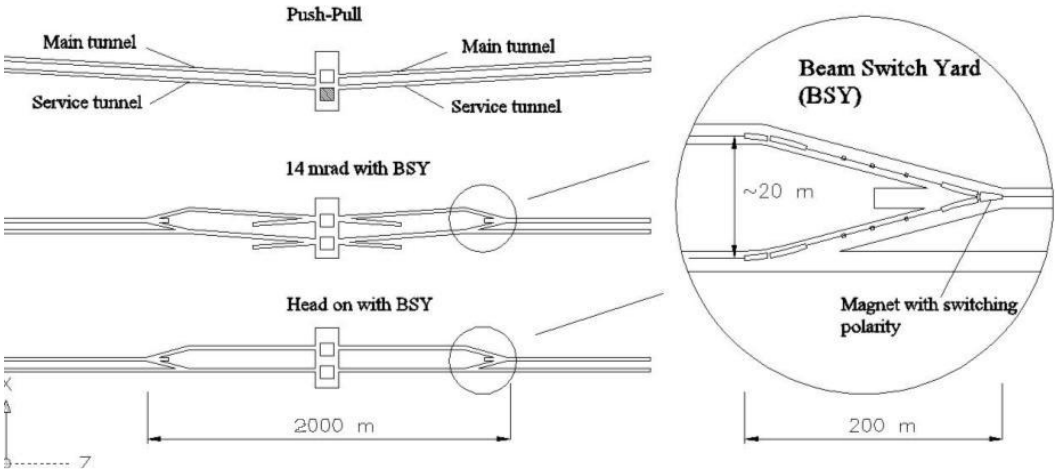

Figure 15. Possible arrangement for simultaneous operation of two detectors.

Other specification reflected in [10] is that the superconducting final doublets, consisting from QD0 and QF1 Quadrupoles (and associated Sextupoles SD0 and SF1) are grouped into two independent cryostats. The cryostat with defocusing quadrupole QD0 penetrates almost entirely into the detector. The QD0 cryostat is specific for the detector design and moves together with detector during push-pull operation, while the QF1 cryostat is common and rests in the tunnel.

This last specification requires clarification, hovewer.

Stability requirements for the lenses of final doublet.

Lenses QF1 and QD0 located at both sides of detector provide each-side beam focus at IP in both transverse directions –*x* and *y*. If however, the quadrupole lens at one side is shifted transversely from its position to the Δx, the beam arriving from this side gets an angular kick which will propagate to the IP. The kick for such displacement can be calculated as

$$\alpha = x' = \frac{e\Delta x \cdot \int G(s)ds}{mc^2\gamma} \cong \frac{\Delta x \cdot G \cdot l}{(HR)} \ , \qquad (7)$$

where $(HR)[Gs \cdot cm] = E[eV]/300$ is so called magnet rigidity of the high energy beam, *l* stands for effective length of the lens, *G*(*s*) describes its longitudinal field distribution with maximal gradient *G* at the center. For $300GeV$ beam magnetic rigidity comes to $(HR) \cong 10^9[G \cdot cm] \equiv 10^6[kG \cdot cm] \equiv 10^3[T \cdot m]$, $\gamma \cong 6 \cdot 10^5$.

Propagation of kick $x'(s_0) = \alpha$ from its origin at the lens location s_0 to the IP located at s_1 counted from the lens's center, described by sin-like trajectory $S(s,s_0)$ having starting point at the lens location s_0

$$x(s_1) = x_0'(s_0)S(s_1, s_0) = \alpha \cdot S(s_1, s_0), \qquad (8)$$

where $S(s_0, s_0) \equiv S(s_0) = 1$, $\boldsymbol{\alpha}$ is a kick angle; with similar equation for the other transverse coordinate *y* if kick happen in other direction too. By introduction of usual envelope function and the phase change as

$$\Delta\Phi \equiv \Delta\Phi_x(s_1, s_0) = \int_{s_0}^{s_1} ds / \beta_x(s), \tag{9}$$

displacement and the slope of the beam centroid at the IP come to

$$x(s_1) = \alpha\sqrt{\beta_x(s_1)\beta_x(s_0)}Sin(\Delta\Phi), \quad x'(s_1) = \alpha\sqrt{\frac{\beta_x(s_0)}{\beta_x(s_1)}}\left[Cos(\Delta\Phi) + \tfrac{1}{2}\beta_x'(s_1)Sin(\Delta\Phi)\right] \tag{10}$$

where $\beta_x(s_1), \beta_x(s_0)$ stand for envelope functions values at the IP and at the lens respectively (for other coordinate, *y*, the functions are $\boldsymbol{\beta}_y(s_1), \boldsymbol{\beta}_y(s_0)$). As the IP is the focusing point for this lens, then $Sin(\Delta\Phi) \cong 1$ as the betatron phase changes to $\Delta\Phi \cong \pi/2$ during transformation to IP.

If displacement is bigger, than the transverse beam size of incoming bunch (which is between 3.5–9.9 *nm*, according to BDR), beams do not collide, so the requirement for the displacement at IP comes to

$$\sqrt{\frac{\gamma\varepsilon_x \cdot \beta_x(s_1)}{\gamma}} > \alpha\sqrt{\beta_x(s_1)\beta_x(s_0)}, \tag{11}$$

where $\boldsymbol{\gamma\varepsilon}_{x,y}$ stand for invariant emittance for appropriate coordinate (left side is just beam size at IP) . So the restriction for the kick and displacement come to

$$\alpha = \frac{\Delta x Gl}{(HR)} < \sqrt{\frac{\gamma\varepsilon_x}{\gamma\beta_x(s_0)}} \;; \quad \Delta x < \frac{(HR)}{Gl}\sqrt{\frac{\gamma\varepsilon_x}{\gamma\beta_x(s_0)}} = \frac{1}{kl}\Delta x', \tag{12}$$

$\Delta x' = \sqrt{\frac{\gamma\varepsilon}{\gamma\beta(s_0)}}$ –is the angular spread at the location of lens, $k^{-1} = \frac{(HR)}{G}$ –is the lens parameter, and the similar equations for *y*- coordinate. One can see that this restriction is not depending on beta-function value at IP.

Normalized emittance of ILC beam is $\boldsymbol{\gamma\varepsilon}_x \cong 10^{-5} m \cdot rad$, $\gamma\varepsilon_y \cong 4 \cdot 10^{-8} m \cdot rad$, so the vertical jitter emerges as the mostly dangerous. Let us estimate the tolerances for QF1 as if it is based at the tunnel site and its jitter is not correlated with the location of other lenses. For gradient in lens $G \cong 10 kG \cdot cm$, effective length of lens *l*=200*cm*, $\boldsymbol{\beta}(s_0) \cong 10^4 m$, for 300-*GeV* beam energy, the vertical jitter (coordinate *y*) limited to

$$\Delta y < \frac{10^6 [kG \cdot cm]}{10[kG/cm] \cdot 200[cm]}\sqrt{\frac{4 \cdot 10^{-8}[m]}{6 \cdot 10^5 \cdot 10^4 [m]}} \cong 1.3 \cdot 10^{-6} cm \equiv 0.013 \mu m \equiv 13 nm \;.$$

This shift corresponds to the complete miss of bunches i.e. mismatch of the order of the beam transverse beam size sigma, so for partial mismatch this number must be

reduced at least 10 times for 10% reduction of luminosity, coming to restriction of the order $\Delta y_m \leq 1.3nm$.

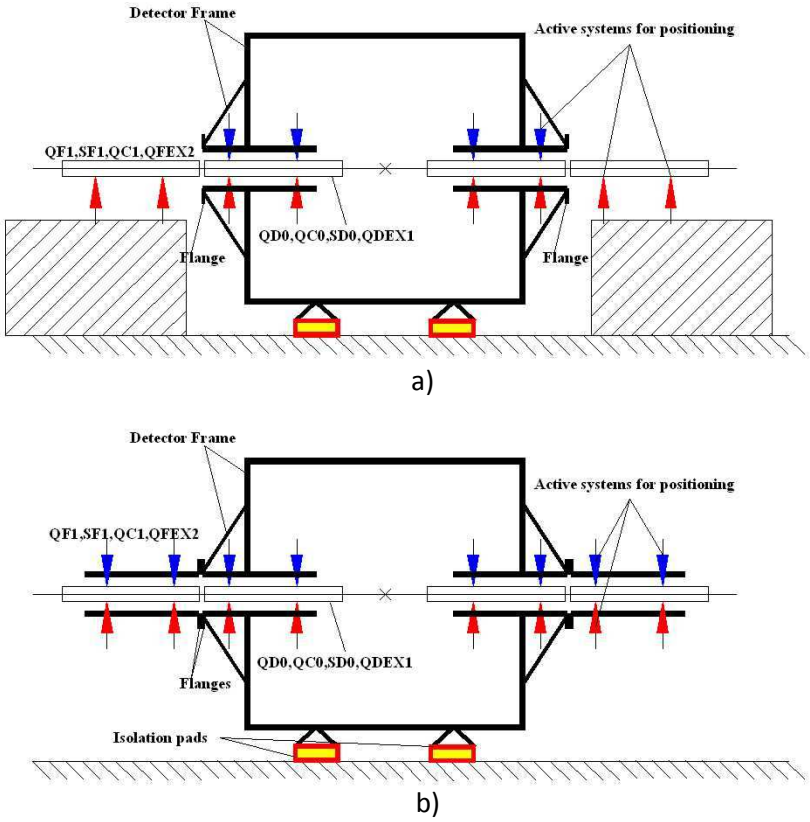

Figure 16. a)- Basement of final doublet in ILC, b)-recommended basement concept.

Indeed, if all lenses participating in beam size formation at both sides of detector move as a whole, this effect does not manifest.

That is why we are suggesting installation of all final lenses at the same frame – common practice in ordinary optics.

The beam based alignment system, accommodated in ILC will operate a dipole trimming coils mounted inside the same cryostat as the lenses, and will provide equivalent shift of lens axis by changing electrical current in its coils as necessary.

That is why we are suggesting basement of final doublet to the detector's frame. This is a common practice in optics: all elements installed of the same (optical) table. Utilization of 2K Helium in final quads cooling can bring <15% increase of field maximum, so we are not considering it for QD0 at the moment, although it might be included later, just widening the margins for safe operation.

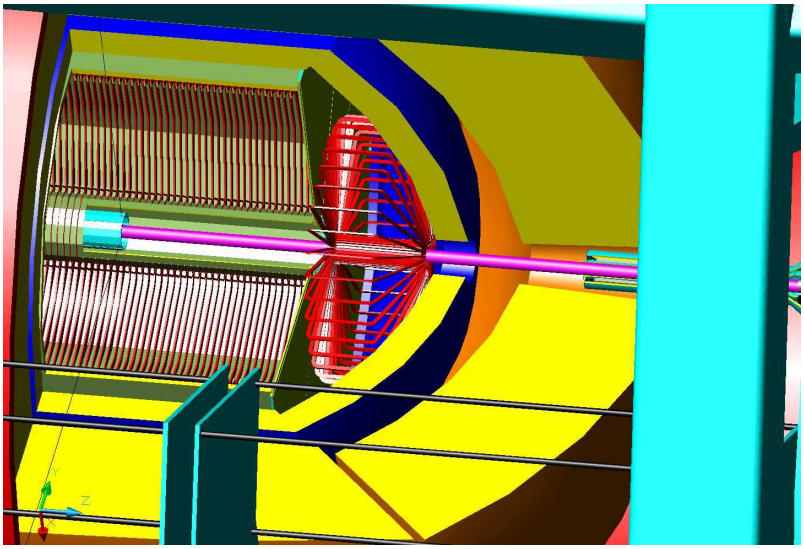

Figure 17. Toroidal coil for improve the momentum resolution for small angles.

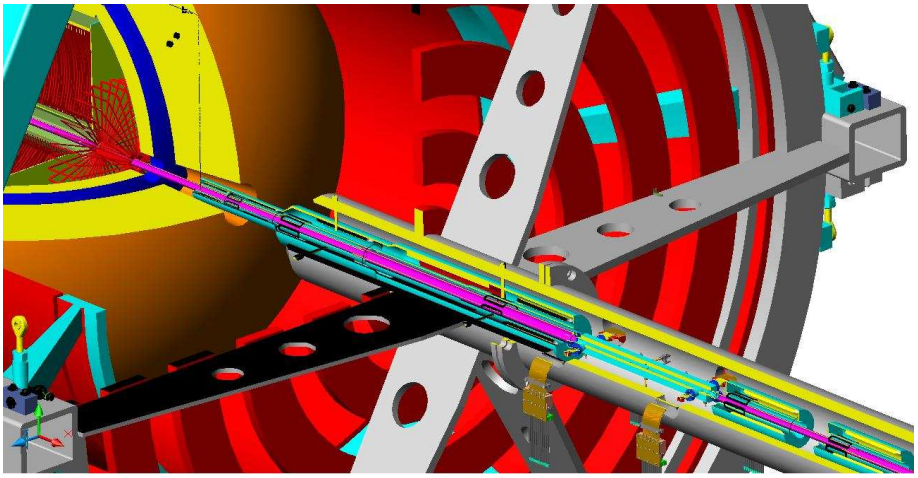

Figure 18. (See Fig.4).

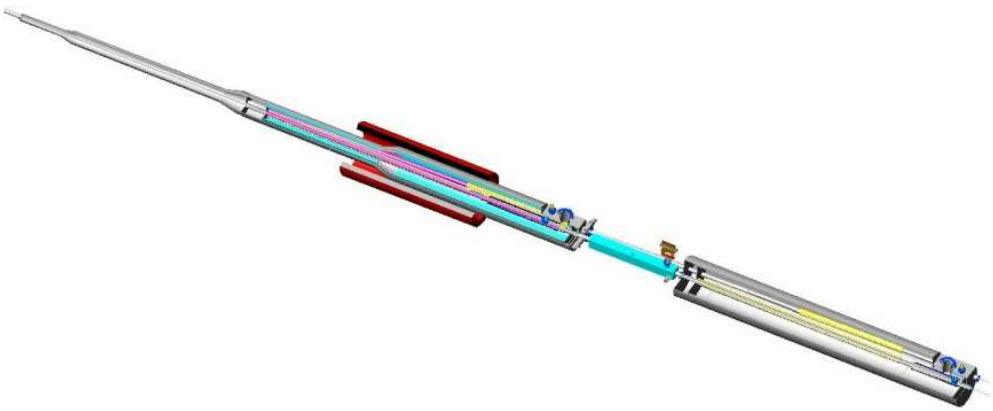

Figure 19. Final doublet with sextupoles, and the kicker (for head-on-collisions).

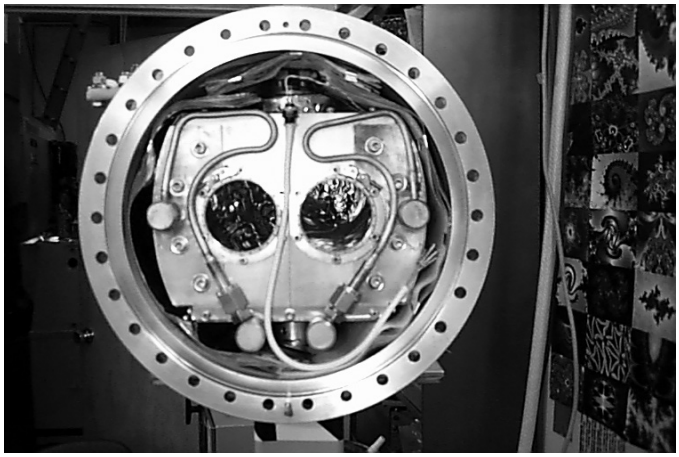

Figure 20. Dual bore quadrupole developed at Cornell.

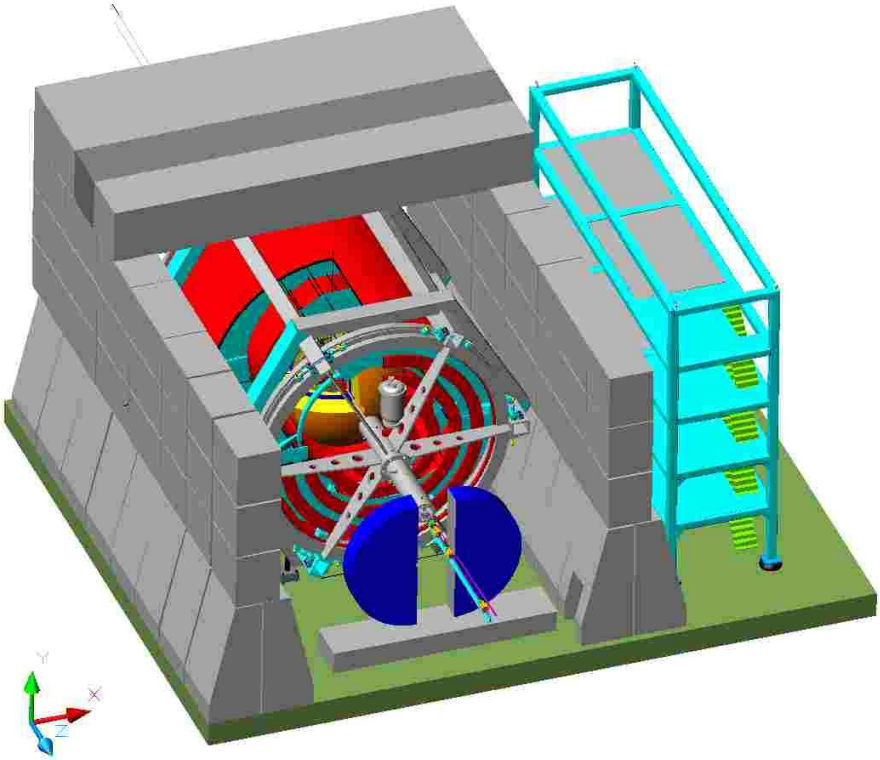

Figure 21. Assembled detector inside Borated Concrete walls, made from separate blocks.

DUAL READOUT CALORIMETER

Dual readout techniques [5]-[8] deal with the time structure analyses of signal from the crystals. Typically it is a fast Cherenkov light output and slower scintillation signal.

Typically, for the gamma and lepton calorimetry, the crystals of BGO ($Bi_4Ge_3O_{12}$) –Bithmuth Germanium Oxide. This inorganic chemical compound is no hygroscopic.

Other dual readout system is a hadronic calorimeter with two (or more) types of fibers having different properties for registration of Cherenkov light and scintillation. Utilzation of (optical) filters allows better identification of Cherenkov light and scintillation one as they have different spectrum. Time structure of signals from BGO is represented in Fig. 22.

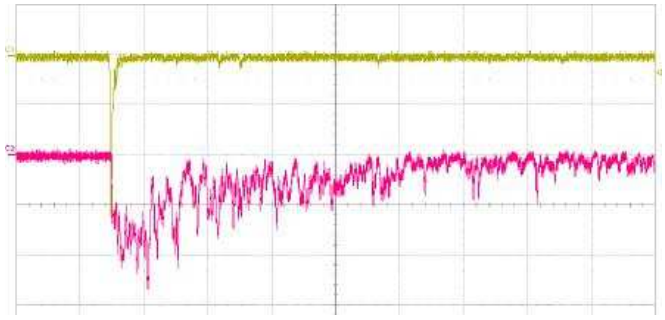

Figure 22. Time structure of Cherenkov signal (upper curve) and scintillation one (lower curve), [5], [9].

So by measurements of signal in two different time gates allows distinguishing between the type of particle.

CLUSTER COUNTING (CluCou)

CluCou is a procedure for measurements the drift times of all electron clusters generated by particle on its way inside the drift tube or wire chamber [3], [9]. For reduction of mass, the wires are made from Carbon wires.

Typical gas mixture contains Helium (90%) with Iso-Butane(10%) HeC_4H_{10}. Wires are made from Carbon composite for lowering the amount of scattering substance. This method allows to reach a spacial resolution higher than the wire granulation.

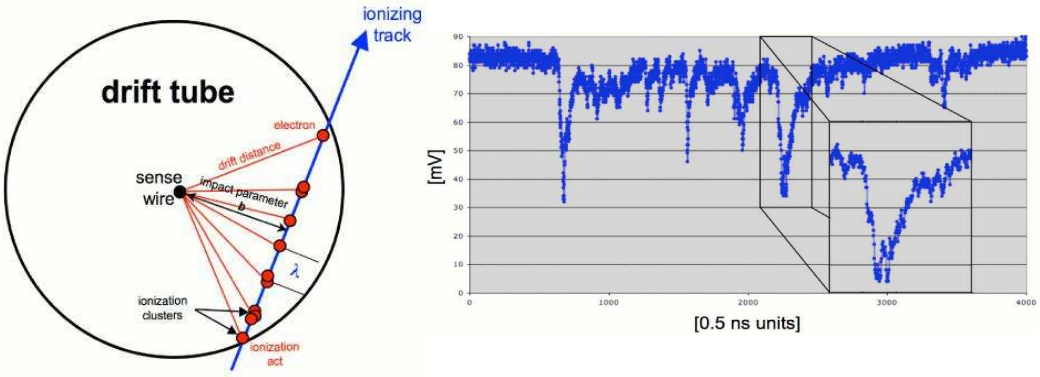

Figure 23. The principle of CluCou. At the left: geometry of drift tube with ionizing track. At the right: the time structure of a signal from drift tube [9].

VERTEX DETECTOR

The vertex detector is a multi Giga-pixel chamber with cylinders and disks [9]. With pixels of ~20 µm, spatial resolution could reach ~5µm. For a pixel size of 20 µm with a dead area of 10 µm along the perimeter of the sensors, the total number of channels comes to 4.3×10^9. In a future these pixel dimensions will be lowered as the technology progresses.

TECHNOLOGY FOR LARGE SOLENOIDS

As we could see, the return field value depends on the ratio of the areas with corresponding flux. So by making the outer solenoid larger, one can reduce the field, required from outer solenoid and in reaching higher field level in the inner solenoid (Less field value is subtracted).

SC cable with 30=2x15 wires diam. 0.8mm each, Current ~18 kA total;
Separation with ribs having thickness 5mm (grooves ~1.5mmx20mm);
Carcasses made from Al alloy;
Thickness of coil in regular section ~6cm;
End section ~50cm x 13cm total in 16 radial sections;
Even if all stored energy (~2.8GJ) disappeared in carcasses, temperature gain ~70^o C;
SC cable fixed in grooves with alloy and by compression;
Sectioned assembling;
Indirect cooling;
In case of quench valves block the Helium supply from the storage;
Outer solenoid is thinner, much relaxed design

Number of turns in main solenoid is ~900x2
Number of turns in outer solenoid is ~441x2

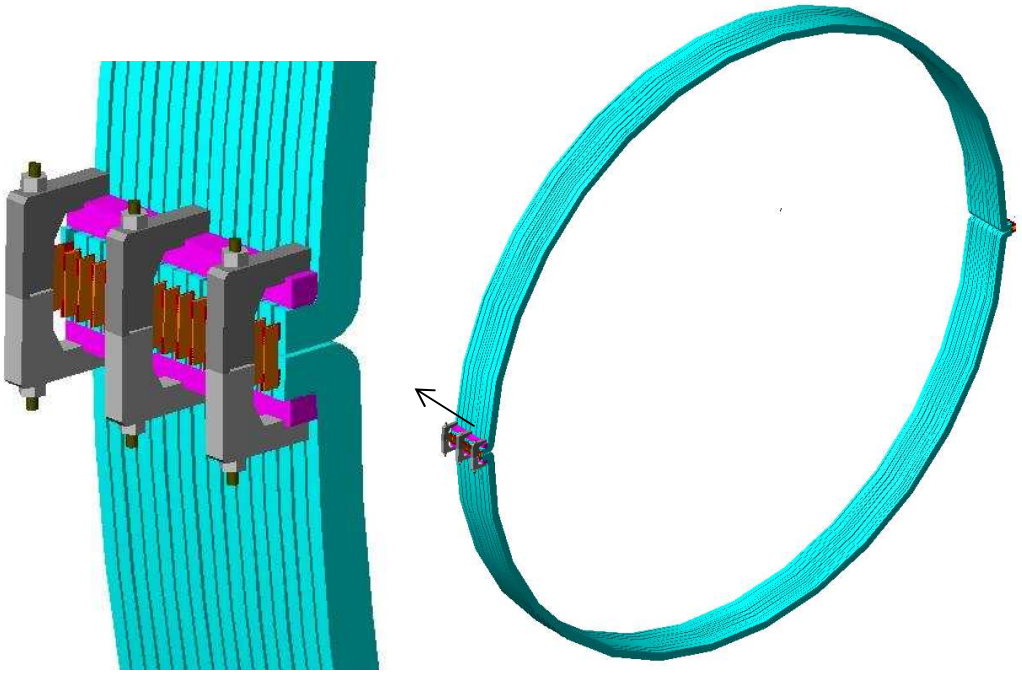

Figure 24. The coil could be split in half.

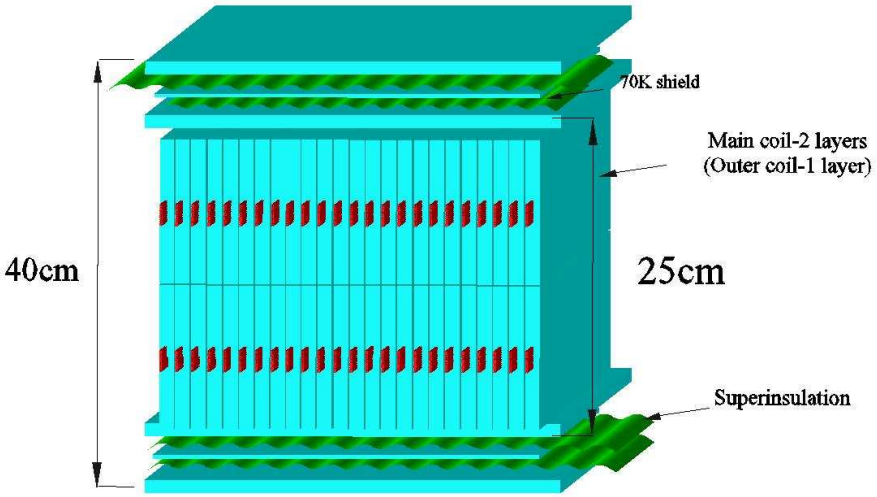

Figure 25. Fragment of coil inside a cryostat.

Dimensions of conductor with Al stabilizer is ~10x1 cm

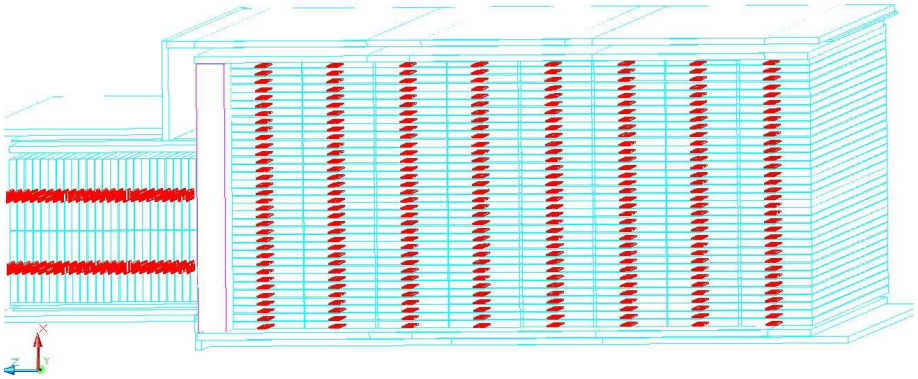

Figure 26. End sections of main solenoid.

This is a traditional approach. Another approach is to solder the Copper matrix into the slits in Al cylinder. The solder and flux for brazing Al with Copper is well known [11].

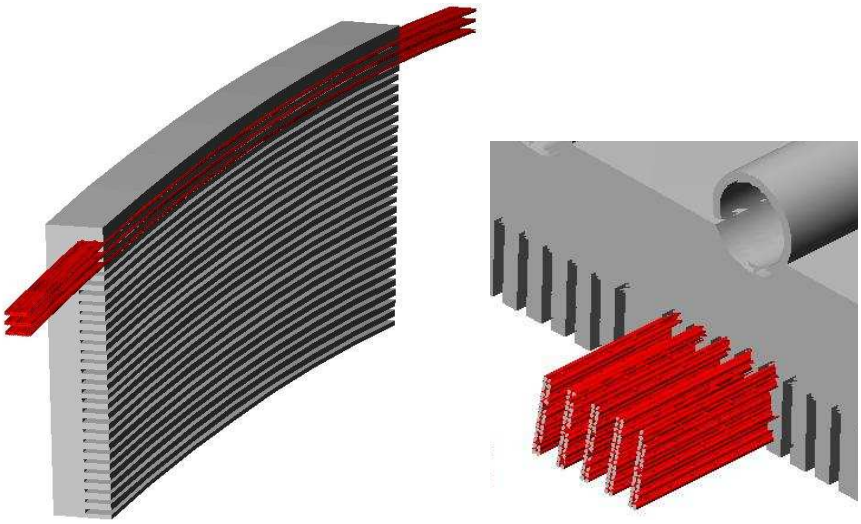

Figure 27. The cable soldered in Aluminum carcasses.

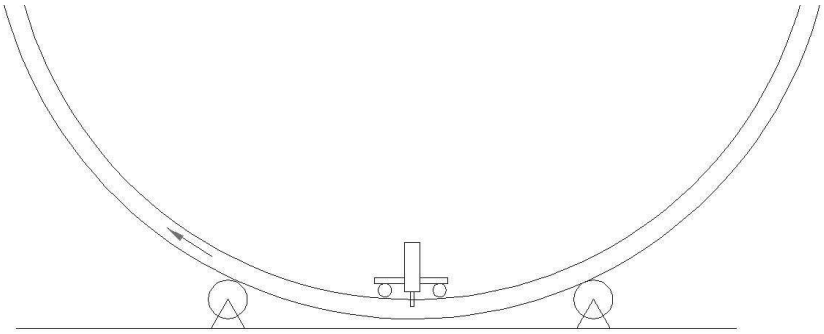

Figure 28. One possibility to make the grooves in a modular coil; Cartridge based to the neighboring grooves.

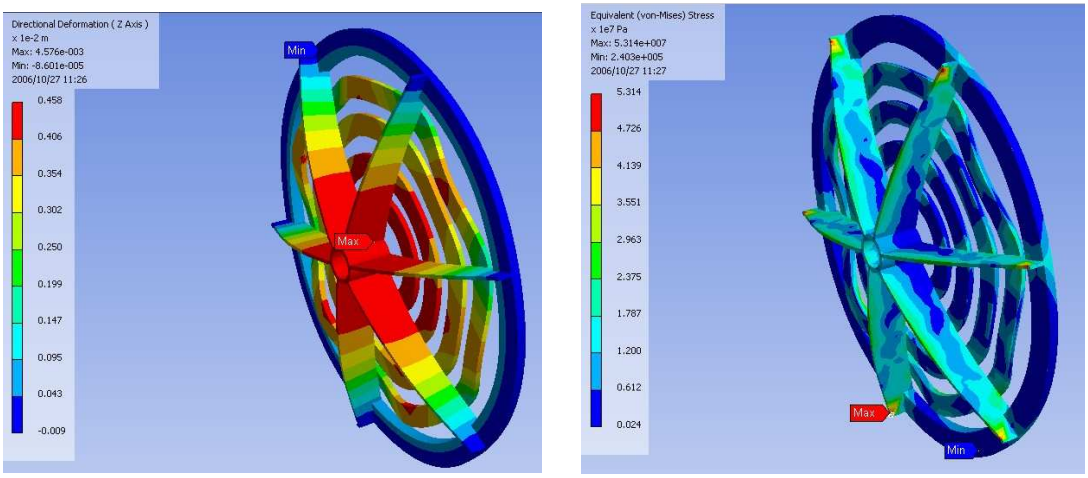

Figure 29. Deformation of frame with end coils [12]. Maximal deformation is 4.57 mm, maximal stress ~5x10^7 Pa.

CONCLUSIONS

So important issues associated with Iron-free detector and implemented in a 4th Concept are:

a) Integration of FF hardware into detector;
b) Any crossing angle OK, but lobby for zero-degree crossing with a kicker with travelling wave and BSY for two IRs;
c) Easy installation and reinstallations;
d) Reverse magnetic field in detector to cancel detector asymmetries, especially important for polarized beams;
e) Numerous experimental conveniences, e.g., surveying, new add-ons or replacements in later years, etc.

We believe that the system with multiple return solenoids is a perspective one, Fig.29 as it allows higher magnetic field on the axis.

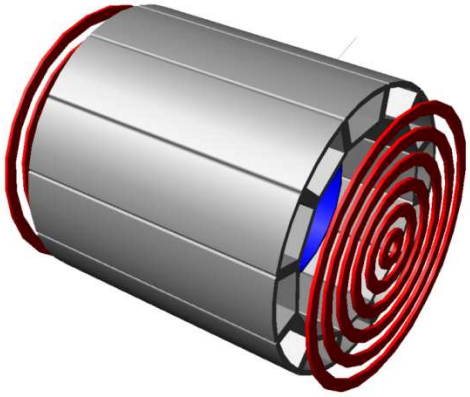

Figure 30. Perspective configurations of detector with many return solenoids.

REFERENCES

[1] A.Mikhailichenko, ”Do Detectors Need a Yoke?”, CBN 01-20, Cornell, LEPP, Oct. 6, 2000, 6pp.

[2] A.Mikhailichenko, ”Detector for Linear Collider”, CBN 02-3, Cornell, LEPP, Oct. 6, 2002, 7pp.

[3] G.Cataldi, F.Grancagnolo, and S.Spagnolo, “Cluster Counting in Helium Based Gas Mixtures,” Nucl. Instrum. and Methods A386 (1997) 458-469.

[4] A.Mikhailichenko, “Particle Acceleration In Microstructures Excited by Laser Radiation”, CLNS 00/1662, LEPP, Cornell, Feb. 11, 2000, 89 pp.

[5] N. Akchurin, K. Carrell, J. Hauptman, H. Kim, H.P. Paar, A. Penzo, R. Thomas, R. Wigmans, “Hadron and Jet Detection with a Dual-Readout Calorimeter”, *Nucl. Instrs. Meths*. A537 (2005) 537-561.

[6] “Electron Detection with a Dual-Readout Calorimeter”, *Nucl. Instrs. Meths.* A536 (2005) 29-51.

[7] “Muon Detection with a Dual-Readout Calorimeter”, *Nucl. Instrs. Meths.* A533 (2004) 305-321.

[8] “Dual-Readout Calorimetry with Lead Tungstate Crystals,” *Nucl. Instrs. Meths.* A584 (2007) 273-284

[9] 4th Concept

[10] B.Parker, A.Herve, J.Osborne, A.Mikhailichenko, K.Buesser, B.Ashmanskas, V.Kuchler, N.Mokhov, A.Enomoto, Y.Sugimoto, T.Tauchi, K.Tsuchiya, J.Weisend, P.Burrows, T.Markiewicz, M.Oriunno, A.Seryi, M.Sullivan, D.Angal-Kalinin, T.Sanuki, H.Yamamoto, ”Challenges and Concepts for Design of an Interaction Region with Push-pull Arrangement of Detectors – an Interface Document”, EPAC 08, Genoa, Italy, 2008.

[11] J.Diamond, “Tinning Aluminum wire”, The Review of Sci. Instr., vol 43, No4, 1972,pp702-703.

[12] A.Mikhailichenko, J.Hauptman, “4th Concept MDI Issues and IP design”, Beigin, China LCWS, Feb 5, 2007.